Available online at www.sciencedirect.com
SCIENCE DIRECT®
Journal of Solid State Chemistry 178 (2005) 769–775
JOURNAL OF SOLID STATE CHEMISTRY
www.elsevier.com/locate/jssc

Partial substitution of rhodium for cobalt in the misfit $[Pb_{0.7}Co_{0.4}Sr_{1.9}O_3]^{RS}[CoO_2]_{1.8}$ oxide

Denis Pelloquin, Sylvie Hébert, Antoine Maignan*, Bernard Raveau

Laboratoire CRISMAT, UMR CNRS-ENSICAEN 6508, 6 boulvard du Maréchal Juin, 14050 Caen Cedex, France

Received 31 July 2004; received in revised form 15 November 2004; accepted 19 November 2004

Abstract

The partial substitution of Co by Rh in the $[Pb_{0.7}Co_{0.4}Sr_{1.9}O_3]^{RS}[CoO_2]_{1.8}$ family has been investigated. By transmission electron microscopy and X-ray powder diffraction, it is shown that the substitution of Rh for Co takes place at the two cobalt sites of the structure but for the low enough Rh contents, this substitution is made preferentially at the level of the CdI_2-like layer. Thus, a generic formula $[Pb_{0.7}(Co_{0.4-z}Rh_z)Sr_{1.9}O_3]^{RS}[Co_{1-y}Rh_yO_2]_{b1/b2}$ ($0 \leqslant y \leqslant 0.5$ and $0 \leqslant z \leqslant 0.3$) can be proposed for this new family of misfit phase. As observed for the pure misfit cobaltite, the thermoelectric power is also very large, close to $+140\,\mu V/K$ at room temperature. The Rh cation can adopt a mixed valency Rh^{3+}/Rh^{4+} ($4d^6/4d^5$) with low spin states t_{2g}^6/t_{2g}^5 equivalent to the ones of low spin Co^{3+}/Co^{4+} ($3d^6/3d^5$). The large thermopower observed in the Rh substituted compounds is therefore a direct proof that the coexistence of low spin states t_{2g}^6/t_{2g}^5 contributes to the thermoelectric power enhancement in these oxides.
© 2004 Elsevier Inc. All rights reserved.

Keywords: Cobalt oxide; Thermopower; Rhodium oxide

1. Introduction

The intensive research in the cobalt oxides points out to the great ability of the cobalt species to adopt a mixed valence state and various spin state configurations in different basic structural environments, such as perovskite or CdI_2-type blocks. This richness allows to design some new structural frameworks with interesting physical properties. Among the latter, the thermoelectric properties have been the focus of numerous studies these last years after the discovery of a high thermoelectric power ($\sim 100\,\mu V/K$ at 300 K) and a low resistivity ($\sim 200\,\mu\Omega\,cm$ at 300 K) in $NaCo_2O_4$ [1]. The research for new thermoelectric materials operating at high temperatures ($T \gg 300$ K) is a very interesting challenge since the waste heat conversion into electrical energy is economical and non-polluting. Recently a large oxide series which exhibits hexagonal Co sheets of the CdI_2-type containing edge-shared CoO_6 octahedra—similar to that of $NaCo_2O_4$ [1]—interleaved with three or four rocksalt (RS) type layers has been isolated. These materials, the so-called "misfit" cobaltites due to their aperiodic composite feature, can be described by the generic formula $[(A'_{1-x}Co_y)_{n-2}A_{2+x-y}O_n]^{RS}[CoO_2]_{b1/b2}$ in which n is the number of RS-type layers ($n = 3$ or 4 and A' = Co,Bi, … and A = Ca, Sr) [2–7] and the b_1/b_2 ratio represents the incommensurate ratio of the b parameters of the two subcells.

One possible origin for the large Seebeck coefficient of Na_xCoO_2 is based on the different valencies and spin states the cobalt species can adopt [8]. In the limit of high temperature, the thermopower can be estimated from a generalized Heikes formula, which takes into account the carrier density as well as their spin degeneracy (low spin, intermediate spin or high spin). A mixture of low spin Co^{3+} and low spin Co^{4+} (t_{2g}^6/t_{2g}^5) was proposed to be at the origin of the large thermoelectric power observed at high temperature in Na_xCoO_2. For misfit cobaltites, the same explanation can be given to explain their good thermoelectric properties and the improvement that can be achieved by different

*Corresponding author. Fax: +33 2 31 95 16 00.
E-mail address: antoine.maignan@ensicaen.fr (A. Maignan).

0022-4596/$ - see front matter © 2004 Elsevier Inc. All rights reserved.
doi:10.1016/j.jssc.2004.11.021

substitutions [9]. By magnetic measurements [4] and photoemission studies [10], the coexistence of low spin Co^{3+}/low spin Co^{4+} in the CoO_2 layers has been proposed. One way to demonstrate the importance of the mixture of low spin Co^{3+}/low spin Co^{4+} to achieve large Seebeck coefficient is by substituting an isoelectronic element for Co in the CoO_2 layer.

The difficulty with substitution in misfit cobaltites is that two different Co sites can be substituted, in the RS layers or in the CoO_2 layers. Recently, different substitutions at the level of RS layers have been reported in such type of oxides. In particular, the strontium substitution for calcium in $Ca_3Co_4O_9$, namely $[Co Ca_2O_3]^{RS}[CoO_2]_{1.62}$, has been made [11,12] and the possibility to introduce partially lead [9,13], mercury [13,14] or lanthanides [15] instead of cobalt in the rock–salt type layers has been demonstrated. By this way a significant enhancement of the RT thermopower has been reported in $[Pb_{0.4}Co_{0.6}Ca_2O_3]^{RS}[CoO_2]_{1.61}$ with the highest value of 165 μV/K [9]. The substitutions reported with transition elements has led to the synthesis of $[Ti_{0.4}Co_{0.6}Ca_2O_3][CoO_2]_{1.62}$ [16] and $[Ca_2(Co_{0.65} Cu_{0.35})_2O_4][CoO_2]_{1.60}$ [17], two new $n = 3$ and 4 misfit cobaltites, respectively. All copper or titanium species are located in the RS-type subcell and do not directly modify the conducting $[CoO_2]$-type CdI_2 layers.

In the case of $NaCo_2O_4$, substitutions with Cu [18], Pd [19] or Mn [20] for Co have been reported. Even if the physical properties are modified, no definite proof that the substitution takes place only in the CoO_2 layer has been given.

A new attempt to modify the CoO_2 layers in misfit cobalt oxides is presented here. According to a similar filling of the *d* orbitals for $Co^{3+/4+}$ ($3d^6$,$3d^5$) and $Rh^{3+/4+}$ ($4d^6$,$4d^5$) and to the stability of the low spin state of the latter [21], the rhodium species appear to be a promising candidate to substitute the cobalt species. Here we report on different levels of rhodium substitution for cobalt in the lead-based $[Pb_{0.7}Co_{0.4}Sr_{1.9}O_3]^{RS}[CoO_2]_{1.8}$ misfit cobaltite. The structural characterizations by transmission electron microscopy (Electron Diffraction + Energy Dispersive Spectroscopy) and powder X-ray diffraction data are reported and evidence large rhodium substitution for cobalt. Such analytical results imply the partial substitution of cobalt species sitting in the CdI_2-type layers. The thermopower properties are given and compared with the previously reported pure $[(A'_{1x}Co_y)_{n-2}A_{2+x-y}O_n]^{RS}[CoO_2]_{b1/b2}$ cobaltites. The large thermoelectric power values emphasize the importance of low spin Co^{3+}/Co^{4+} mixture in the CoO_2 layers to achieve large Seebeck coefficients.

2. Experimental

The synthesis of the polycrystalline samples is similar to the method used in the case of Pb-based misfit cobaltites [9,13]. Stoichiometric amounts of oxides and peroxides, Rh_2O_3, PbO, SrO_2 and Co_3O_4 are weighted according to the nominal cation composition $Pb_{0.7}Sr_{1.9}Co_{2.2-x}Rh_xO_y$, deduced from the structural study of the pure cobalt $[Pb_{0.7}Co_{0.4}Sr_{1.9}O_3]^{RS}[CoO_2]_{1.8}$ oxide. Note that the Rh_2O_3 oxide is kept for one night at 1000 °C to avoid the presence of water molecules. Then the precursors are mixed and pressed in the form of bars. The samples are placed in silica tubes sealed under vacuum with approximately 0.8 g of sample for a volume of 3 cm^3 in the tube. The samples are heated up to 1000 °C with a heating rate of 150 °C/h, maintained at this temperature for 24 h and cooled down to room temperature at the same cooling rate. By this way, pressure is observed inside the tubes and black ceramic bars are obtained.

Next the as-prepared samples are analyzed by means of transmission electron microscopy (TEM) techniques. The electron diffraction (ED) analysis has been carried out using a JEOL 200CX microscope fitted with an eucentric goniometer ($\pm 60°$) and equipped with KEVEX Energy Dispersive Spectroscopy (EDS) analyzer. The accuracy of this analysis technique is about 5/100 for each cation.

X-ray diffraction data are collected at room temperature using an XpertPro Philips vertical diffractometer working with the Cu$K\alpha$ radiation and equipped with a secondary graphite monochromator. Data collection is carried out by continuous scanning (step = 0.02° (2θ), preset = 10 s) over an angular range $5° \leqslant 2\theta \leqslant 80°$. Lattice constants and structural calculations were refined by the Rietveld method using the computer programs JANA2000 [22] and FULLPROF [23], respectively.

The magnetic properties are studied using a SQUID magnetometer (ac and dc; 0–5 T; 1.8–400 K). Resistance data as a function of temperature (1.8–400 K) or magnetic field (0–7 T) are collected with a Quantum Design physical properties measurement system (PPMS) by the four-probe technique. Current and voltage indium contacts are ultrasonically deposited on the sintered bars (typically $2 \times 2 \times 10$ mm). A steady state method is used to measure the Seebeck effect (S) in the PPMS with high temperature limit fixed at 320 K by the calibration range of the temperature sensors.

3. Structural analysis

The samples have been prepared on the basis of the chemical formula previously reported for the Pb-based misfit oxide, $[Pb_{0.7}Co_{0.4}Sr_{1.9}O_3]^{RS}[CoO_2]_{1.8}$ [13]. In order to simplify this formula, especially if one takes into account that the location of the Rh cations in the RS and/or the CdI_2 type layers is a priori unknown, the formula can be written $Pb_{0.7}Sr_{1.9}Co_{2.2}O_{6.6}$. A series of

the sample has been prepared by substituting rhodium for cobalt leading to the formula $Pb_{0.7}Sr_{1.9}Co_{2-x}Rh_xO_y$ by $\Delta x = 0.3$ steps. The corresponding X-ray powder diffraction patterns (Fig. 1) reveal a great analogy with the data reported for the $[Pb_{0.7}Co_{0.4}Sr_{1.9}O_3]^{RS}[CoO_2]_{1.8}$ phase [13] and for x values larger than 0.9, they show the presence of an impurity which is isostructural to $Sr_6Co_5O_{15}$ [24]. For $x > 1.5$, multiphasic samples are obtained without obvious traces of a misfit-related phase.

In order to check the structural relationships with the $[Pb_{0.7}Co_{0.4}Sr_{1.9}O_3]^{RS}[CoO_2]_{1.8}$ misfit cobaltite and to establish the solubility limit of Rh for Co in such a structure, a TEM study has been made. Some characteristic [100] and [001] oriented ED patterns recorded for the nominal $Pb_{0.7}Sr_{1.9}Co_{1.5}Rh_{0.9}O_{7.67}$ ($x = 0.9$) compound are shown in Fig. 2. The coexistence of two monoclinic sublattices having the same (a,c) crystallographic plane is observed up to $x = 1.5$. Both subsystems, denoted S_1 and S_2, exhibit the following parameters:

$S_1\{a_1 \approx 5\,\text{Å},\ b_1 \approx 5\,\text{Å},\ c_1 \approx 11.5\,\text{Å}$ and $\beta_1 \approx 98^\circ\}$,

$S_2\{a_2 \approx 5\,\text{Å},\ b_2 \approx 2.8\,\text{Å},\ c_2 \approx 11.5\,\text{Å}$ and $\beta_2 \approx 98^\circ\}$, and

a b_1/b_2 misfit parameter ranging from 1.80 (Rh free) to 1.65 depends on the Rh content. The same condition of reflections hkl: $h+k = 2n$, related to a C-type sublattice, is observed for both subsystems in agreement with the previous observations in similar misfit cobaltites [4–7]. However, the coupled EDS analyses for the rhodium richest composition ($x = 1.5$) reveal a maximum Rh content of $x_{EDS} \approx 1.15$, suggesting that this value corresponds to the solubility limit. Moreover, the incommensurability ratio, b_1/b_2, depends on the Rh content going from $b_1/b_2 = 1.8$ for the Rh free sample to $b_1/b_2 = 1.65$ for the sample corresponding to $x_{EDS} = 1.15$, respectively. This demonstrates clearly that the rhodium substitution for cobalt affects the structural properties.

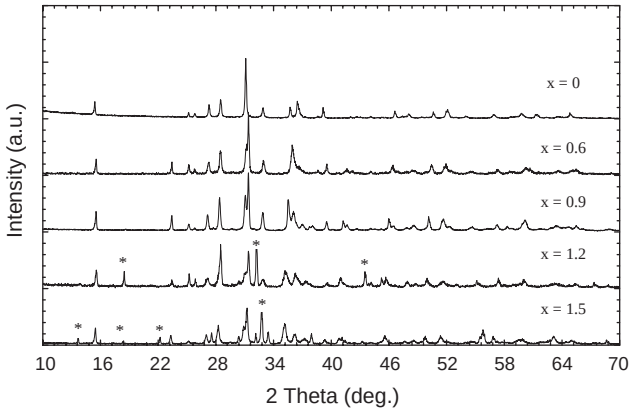

Fig. 1. Experimental powder X-ray diffraction data recorded for the nominal $Pb_{0.7}Sr_{1.9}Co_{2.2-x}Rh_xO_y$ samples with x ranging from 0 to 1.5. Peaks ascribed to the impurities are pointed out by the asterix.

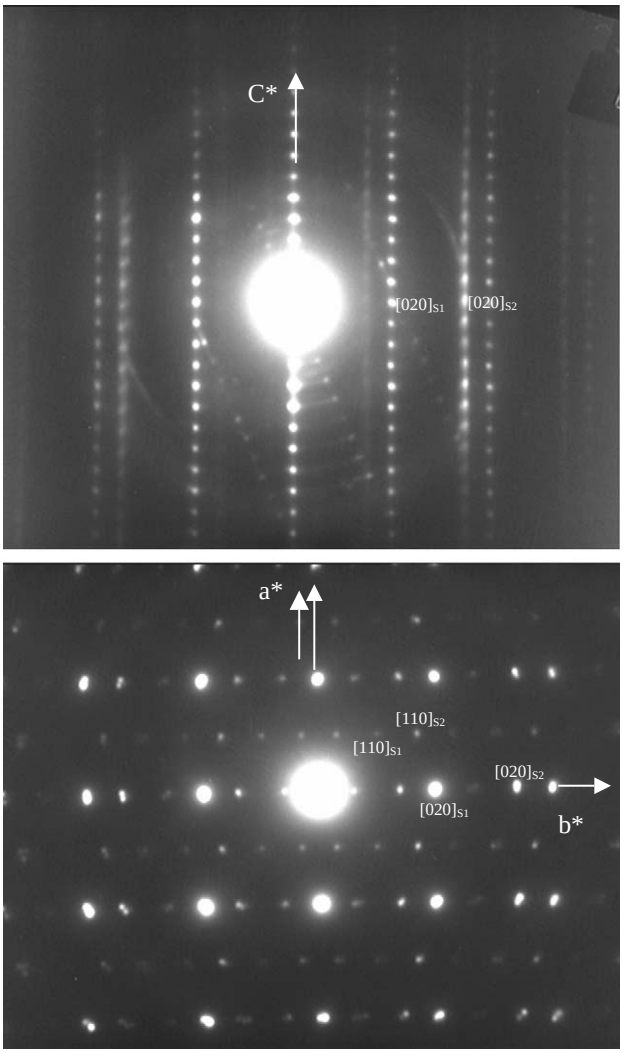

Fig. 2. Experimental (a) [100] and (b) [001] electron diffraction patterns recorded for the nominal sample $Pb_{0.7}Sr_{1.9}Co_{1.3}Rh_{0.9}O_y$ ($x = 0.9$).

By considering those preliminary results, the structural study has been thus limited to the nominal compositions corresponding to $x \leqslant 1.2$ in the $Pb_{0.7}Sr_{1.9}Co_{2.2-x}Rh_xO_y$ chemical formula. The actual chemical composition and the corresponding cell parameters (Table 1) show clear changes compared to the pure cobalt misfit ($x = 0$). Nonetheless, by combining the cation content analyses and the experimental values of the b_1/b_2 ratio given in Table 1, the chemical formulas cannot be written in the "misfit" type with two sublattices, since the location of the Rh in the two different types of layer is unknown. As shown in Table 1, the cobalt content reaches $x_{EDS} \approx 0.85$ for the $x = 0.9$ nominal composition, and taking into account the analyzed Pb and Sr contents, 0.6 and 1.9, respectively, it is obvious that part of the rhodium is substituted in

Table 1
Cell parameters evolution in the $Pb_{0.7}Sr_{1.9}Co_{2.2-x}Rh_xO_y$ misfit system

Nominal compositions	Actual cationic composition		a(Å)	b_1(Å)	c(Å)	b_2(Å)	β(°)	b_1/b_2
	EDS	XRD						
$x = 0$ Ref. [13]	$Pb_{0.66}Sr_2Co_{2.14}$	$Pb_{0.58}Sr_{2.12}Co_{2.10}$	4.938(1)	5.023(1)	11.525(1)	2.802(1)	97.81(1)	1.79(5)
$x = 0.6$	$Pb_{0.60}Sr_{1.9}Co_{1.70}Rh_{0.60}$	$Pb_{0.59}Sr_{1.83}Co_{1.62}Rh_{0.70}$	5.014(1)	4.980(1)	11.503(1)	2.86(1)	97.94(1)	1.744(1)
$x = 0.9$	$Pb_{0.60}Sr_{1.9}Co_{1.39}Rh_{0.84}$	$Pb_{0.67}Sr_{1.76}Co_{1.47}Rh_{0.80}$	5.066(1)	4.974(1)	11.512(1)	2.907(8)	97.98(1)	1.711(1)
$x = 1.2$	$Pb_{0.52}Sr_{2.07}Co_{1.09}Rh_{1.01}$	$Pb_{0.60}Sr_{2.06}Co_{1.00}Rh_{0.97}$	5.117(1)	4.941(1)	11.515(3)	2.96(1)	97.85(2)	1.669(2)
$x = 1.5$	$Pb_{0.68}Sr_{1.99}Co_{0.82}Rh_{1.15}$	Multiphasic	—	—	—	—	—	—

the $[CoO_2]$ layers corresponding of the CdI_2-type sublattice.

The HREM study has allowed to confirm the stacking mode in these misfit structures. This point is illustrated by the $[110]_{RS}$ oriented image shown in Fig. 3a. Triple rows of staggered bright dots, spaced by 3.70 Å along $[1\,\bar{1}\,0]_{RS}$ direction and correlated to triple RS layers, are separated along $\vec{c}$-axis by single rows of diffuse gray dots ascribed to the $[(Co, Rh)O_2]$ layers. In order to check the composition of the different layers, Rietveld analyses have been performed from powder X-ray diffraction data of the three selected samples corresponding to $x = 0.6$, 0.9 and 1.2. From these data by starting from the atomic model (Fig. 3b) used to solve the structure of $[Pb_{0.7}Co_{0.4}Sr_{1.9}O_3]^{RS}[CoO_2]_{1.8}$ [13] and using the super space group $C2/m(1\beta0)s0$ which extrapolates in a 4D formalism the reflection conditions deduced from the ED patterns analysis to take into account the composite feature [14], the cell parameters evolution with the Rh content is obtained (Table 1). It is observed that the a cell parameter increases gradually as the Rh content increases, whereas the b_1 and b_1/b_2 values decrease. The evolution of the stacking parameter is difficult to comment since the Sr/Pb ratio changes slightly as the Rh content increases. In contrast, the b_2 parameter related to the CdI_2-type subcell increases significantly as the Rh content increases. The parameter obtained for Rh richest composition, $b_2 = 2.96$ Å, is clearly greater than $b_2 = 2.80$ Å in the case of the Rh free misfit cobaltite and tends toward that reported for the $SrRh_2O_4$ compound, 3.06 Å, built from Rh-pure CdI_2-type RhO_2 layers [24]. This significant expansion of the a_2 and b_2 cell parameters of the CdI_2-type layer is consistent with the Rh substitution in this layer. The larger Rh^{3+}/Rh^{4+} ionic radii than those of low spin Co^{3+}/Co^{4+} species [25] explains this subcell expansion.

Indeed, for the $x = 0.9$ nominal compound, the refinement of the occupation site of the cation sitting in the CdI_2-type subcell implies to introduce a mixed site in which Rh and Co species are statistically distributed. The refinement of this occupation site leads to a value close to 1.1 for the ratio Co/Rh. This point is illustrated by Table 2 in which final atomic positions and distributions obtained in the case of $x = 0.9$ sample are given. Significant reliability factors, $R_{obs} = 5.23\%$

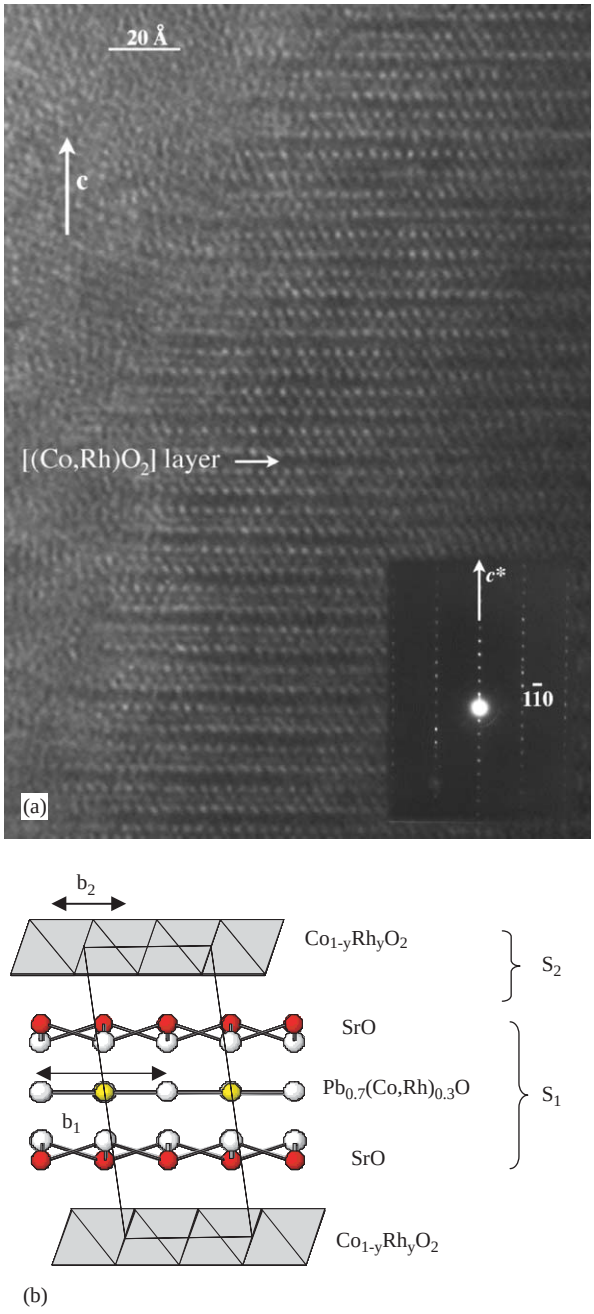

Fig. 3. (a) Experimental [110] oriented HREM image recorded ($\Delta f \approx -500$ Å) for the nominal sample $Pb_{0.7}Sr_{1.9}Co_{1.0}Rh_{1.2}O_y$ ($x = 1.2$) and (b) structural model of the $[Pb_{0.7}(Co_{0.4-z}Rh_z)Sr_{1.9}O_3]^{RS}[Co_{1-y}Rh_yO_2]_{b1/b2}$ misfit cobaltites.

Table 2
Refined atomic positions and main atomic distances for the $x = 0.9$ nominal composition

Space group $C2/m(1\beta0)s0$						Selected interatomic distances (Å)	
Atoms	x	y	z	n	B_{iso}(Å^2)	Sr/Pb(1)–O(1)	2.65(2)
							2.56(1)
Composite part 1 (RS-type)							
Sr	0.4340(9)	0.0	0.2749(3)	1.76(1)	1.2(1)	Sr/Pb(1)–O(2)	2.55(2)
							2.57(2)
Pb(1)	0.4340(9)	0.0	0.2749(3)	0.24(1)	1.2(1)	Sr/Pb(1)–O(3)	2.46(1)
							2.57(1)
							2.63(1)
							2.53(1)
Pb(2)	0.0	0.0	0.5	0.43(1)	0.1(1)	Pb(2)/Co(1)–O(1)	1.99(2)
							1.98(2)
Co(1)	0.0	0.0	0.5	0.57(1)	0.1(1)		
O(1)	0.0	−0.5	0.5	1[a]	1[a]	Pb(2)/Co(1)–O(2)	2.49(2) × 2
							2.53(2) × 2
O(2)	0.060(5)	0.0	0.680(2)	2[a]	1[a]		
Composite part 2 (CdI_2-type)							
Co(2)	0.75	0.75	0.0	0.53(1)	0.0(1)	Co(2)/Rh–O(3)	1.94(1) × 4
Rh	0.75	0.75	0.0	0.47(1)	0.0(1)		1.96(2) × 2
O(3)	0.389(5)	0.75	−0.085(2)	2[a]	1[a]		

The corresponding misfit formula can be written $[Pb_{0.67}Co_{0.57}Sr_{1.76}O_3]^{RS}[Co_{0.53}Rh_{0.47}O_2]_{1.71}$; $R_{obs} = 5.23\%$; $R_{wobs} = 5.53\%$.
[a]Not defined.

and $R_{wobs} = 5.53\%$, for all the observed reflections, are obtained. They are illustrated by the final plot shown in Fig. 4. From this result, the corresponding misfit formula $[Pb_{0.67}Co_{0.57}Sr_{1.76}O_3]^{RS}[Co_{0.53}Rh_{0.47}O_2]_{1.71}$ can be given. This formula can also be written $Pb_{0.67}Sr_{1.76}Co_{1.49}Rh_{0.80}O_{6.42}$. The main atomic distances deduced from this refinement are listed in Table 2.

Interestingly, the refinements up to $x = 0.9$ show that the majority of Rh species is located at the level of the CdI_2-type layer. Beyond $x > 0.9$ some Rh species must be also introduced at the level of the RS-type sublattice to improve the reliability factors. For $x = 1.2$, the resulting occupation values are 0.20(2) Rh species in the rock salt-type layers and 0.80(1) Rh species in the CdI_2-type layer. Nevertheless, this result must be given cautiously since the quality of the X-ray data decreases with the formation of $Sr_6(Co,Rh)_5O_{15}$ as a secondary phase for $x \geqslant 0.9$. From all these different refinements, it appears that in the CdI_2-type sublattice, the Rh substitutes Co to a limit of about 50%, i.e. an average x value close to 0.85. However, it must also be emphasized that the chemical EDS results evidence the possibility to introduce up to 1.15 Rh species in the misfit structure. Thus using the formula proposed for all the misfit cobaltites [6] and taking into account the misfit b_1/b_2 ratio, the generic formula $[Pb_{0.7}(Co_{0.4-z}Rh_z)Sr_{1.9}O_3]^{RS}[Co_{0.5}Rh_{0.5}O_2]_{b1/b2}$ $(0 \leqslant z \leqslant 0.3)$ can be proposed for the rhodium richest samples.

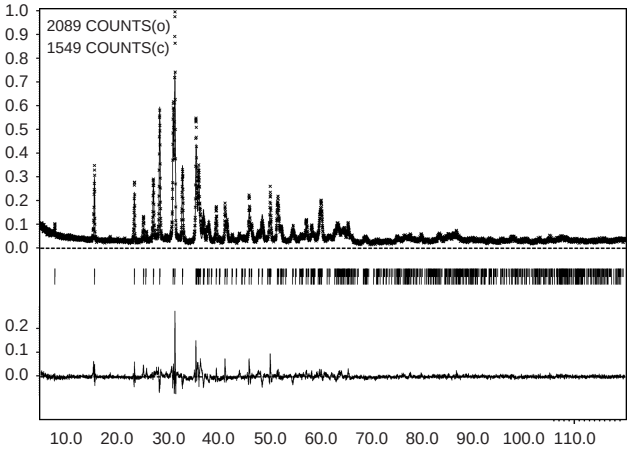

Fig. 4. Experimental, calculated and difference X-ray diffraction patterns corresponding to the $[Pb_{0.67}Co_{0.57}Sr_{1.76}O_3]^{RS}[Co_{0.53}Rh_{0.47}O_2]_{1.71}$ misfit oxide. The vertical bars (upper and lower) are the bragg angle positions of RS and CdI_2-type composite parts, respectively.

4. Transport properties

Fig. 5 presents the thermopower and resistivity as a function of temperature for the $[Pb_{0.7}Co_{0.4}Sr_{1.9}O_3]^{RS}[CoO_2]_{1.80}$ and for $[Pb_{0.67}Co_{0.57}Sr_{1.76}O_3]^{RS}[Co_{0.53}Rh_{0.47}O_2]_{1.71}$ misfit phases. As plotted in the inset of Fig. 5, the resistivity of $[Pb_{0.67}Co_{0.57}Sr_{1.76}O_3]^{RS}[Co_{0.53}Rh_{0.47}O_2]_{1.71}$ is much larger than that of the

Rh-free sample. In addition, it is insulating in the whole temperature range presented here, in contrast with the metallic behavior observed for $T > 100$ K in the Rh-free sample. Compared to other misfit cobaltites, the resistivity is thus strongly increased by the substitution of Rh by a factor close to 10, and the metallicity is destroyed. However, as we are dealing with ceramic samples, this behavior might not reflect the intrinsic properties of this phase and can be strongly affected by the grain boundaries contribution.

As our setup for thermopower measurements is limited to resistivity smaller than $10^4\,\Omega$ cm, the thermopower data are restricted to $T > 100$ K. In the Rh-free compound, S is close to $+115\,\mu$V/K at room temperature and S slightly decreases as T increases from 150 K. For the Rh substituted compound, the shape is slightly different, with a stronger dependence on T, i.e. a larger dS/dT coefficient from 100 to 300 K. The most interesting result is that with Rh substitution, the Seebeck coefficient is very large, close to $+140\,\mu$V/K at 300 K, and is increasing as T increases. One way to explain the large S was proposed by Koshibae et al. [8]. Using a generalized Heikes formula, the high temperature S is given by

$$S = -\frac{k_B}{e} \ln\left(\frac{g_3}{g_4}\frac{x}{1-x}\right)$$

with g_3 and g_4 being the spin degeneracy associated to Co^{3+} and Co^{4+} and x the Co^{4+} concentration. The large S is mainly due to the entropy term arising from the spin degeneracy. In these misfit cobaltites, Co^{3+} and Co^{4+} are reported to be both in the low spin (LS) state in the CoO_2 layers [10] inducing a 1/6 value for g_3/g_4. Since the Rh^{3+}/Rh^{4+} ($4d^6/4d^5$) cations possess similar electronic configurations to the Co^{3+}/Co^{4+} ($3d^6/3d^5$) ones and the Rh^{3+}/Rh^{4+} cations are reported to exist only in the LS state, the fact that the Seebeck coefficient is not strongly affected by a substitution of Rh for Co provides a direct evidence for the role of the LS Co^{3+}/Co^{4+} (t_{2g}^6/t_{2g}^5) electronic configuration to achieve large Seebeck coefficients.

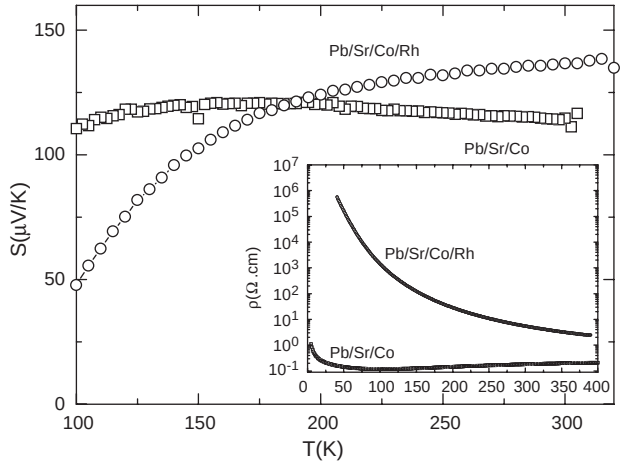

Fig. 5. Thermopower versus temperature for $[Pb_{0.7}Co_{0.4}Sr_{1.9}O_3]^{RS}[CoO_2]_{1.8}$ (squares) and $[Pb_{0.67}Co_{0.57}Sr_{1.76}O_3]^{RS}[Co_{0.53}Rh_{0.47}O_2]_{1.71}$ (circles). Inset: resistivity versus temperature for the two samples.

5. Conclusions

By combining transmission electron microscopy coupled to EDS analyses and X-ray powder diffraction, the partial substitution of Rh for Co in the CoO_2 layers of cobalt misfit oxides has been evidenced. Furthermore, even if this substitution mainly takes place in the CoO_2 layer, some Co species sitting in the NaCl-like layer can also be substituted by Rh species for $x \geqslant 0.9$. The obtained formula for this new family of oxides can be written as $[Pb_{0.7}(Co_{0.4-z}Rh_z)Sr_{1.9}O_3]^{RS}[Co_{1-y}Rh_yO_2]_{b1/b2}$ with $0 \leqslant y \leqslant 0.5$ and $0 \leqslant z \leqslant 0.3$. As the Rh content increases, the b_1/b_2 parameter decreases from 1.80 for the Rh-free compound to 1.65 for the Rh-richest ($x_{EDS} = 1.15$).

The thermoelectric power of these Rh-doped compounds is very similar to the one observed in pure Co misfit oxides. At 300 K, the Seebeck coefficient is close to $+140\,\mu$V/K, larger than the $+110\,\mu$V/K observed in the Rh-free sample. Additionally, the T dependence of the Seebeck coefficient (S) changes at RT from $dS/dT > 0$ to $dS/dT < 0$ for the Rh-free and Rh-containing ($x_{EDS} \approx 0.89$) misfit compounds. It had previously been proposed that the large Seebeck coefficient was mainly due to the spin degeneracy associated to the presence of both Co^{3+} and Co^{4+} in the low spin (LS) state in the CoO_2 layer [8]. The presence of Rh in this layer, which can adopt the same t_{2g}^6/t_{2g}^5 electronic states as low Spin Co^{3+} and Co^{4+} cations, directly evidences that the t_{2g}^6/t_{2g}^5 states and possibly the corresponding spin degeneracy of 1/6 are very important to explain the large thermopower of these oxides.

References

[1] I. Terasaki, Y. Sasago, K. Uchinokura, Phys. Rev. B 56 (1997) R12685.
[2] M. Hervieu, Ph. Boullay, C. Michel, A. Maignan, B. Raveau, J. Solid State Chem. 142 (1999) 305.
[3] H. Leligny, D. Grébille, O. Pérez, A.C. Masset, M. Hervieu, B. Raveau, Acta Crystallogr. B 56 (2000) 13–182.
[4] A.C. Masset, C. Michel, A. Maignan, M. Hervieu, O. Toulemonde, F. Studer, B. Raveau, J. Hejtmanek, Phys. Rev. B 62 (2000) 166.
[5] Y. Miyazaki, T. Miura, Y. Ono, T. Kajitani, Jpn. J. Appl. Phys. 41 (2002) 849.
[6] M. Hervieu, A. Maignan, C. Michel, V. Hardy, N. Créon, B. Raveau, Phys. Rev. B 67 (2003) 045112.
[7] A. Maignan, L.B. Wang, S. Hébert, D. Pelloquin, B. Raveau, Chem. Mater. 14 (2002) 1231–1235.

[8] W. Koshibae, K. Tsutsui, S. Maekawa, Phys. Rev. B 62 (2000) 6869.
[9] A. Maignan, D. Pelloquin, S. Hébert, C. Michel, J. Hejtmanek, J. Appl. Phys. 92 (2002) 1964.
[10] T. Mizokawa, L.H. Tjeng, P.G. Steeneken, K. Schulte, G.A. Sawatzky, N.B. Brookes, I. Tsukada, T. Yamamoto, K. Uchinokura, Phys. Rev. B 64 (2001) 115104.
[11] S. Li, R. Funahashi, I. Matsubara, H. Yamada, K. Ueno, S. Sodeoka, Ceramic Int. 27 (2001) 321.
[12] L.B. Wang, A. Maignan, D. Pelloquin, S. Hébert, B. Raveau, J. Appl. Phys. 92 (2002) 124.
[13] D. Pelloquin, A. Maignan, S. Hébert, C. Martin, M. Hervieu, C. Michel, L.B. Wang, B. Raveau, Chem. Mater. 14 (7) (2002) 3100.
[14] D. Pelloquin, A. Maignan, S. Hébert, C. Michel, B. Raveau, J. Solid State Chem. 170 (2003) 374.
[15] I. Matsubara, R. Funahashi, T. Takenchi, S. Sodeoka, J. Appl. Phys. 90 (2001) 462.
[16] A. Maignan, S. Hébert, Li. Pi, D. Pelloquin, C. Martin, C. Michel, M. Hervieu, B. Raveau, Cryst. Eng. 5 (2002) 365.
[17] Y. Miyazaki, K. Kudo, M. Akoshima, Y. Ono, Y. Koike, T. Kajitani, Jpn. J. Appl. Phys. 39 (2000) L531.
[18] I. Terasaki, I. Tsukada, Y. Iguchi, Phys. Rev. B 65 (2002) 195106.
[19] R. Kitawaki, I. Terasaki, J. Phys. Cond. Matt. 14 (2002) 12495.
[20] Y. Ono, R. Ishikawa, Y. Miyazaki, T. Kajitani, J. Phys. Soc. Jpn. 70 (Suppl. A) (2001) 235.
[21] D.Y. Jung, G. Demazeau, Solid Stat. Comm. 94 (1995) 963.
[22] V. Petricek, et al., JANA 2000 software, Institution of the Physics Academy of Science of the Czech Republik, Prague, 2000.
[23] J. Rodriguez-Carvajal, in: J. Galy (Ed.), Collected Abstract of Powder Diffraction Meeting, 1990, p. 127.
[24] A.L. Hector, W. Levason, M.T. Weller, Eur. J. Solid State Inorg. Chem. 35 (1998) 679.
[25] R.D. Shannon, Acta Cryst. 32 (1976) 751.